Ressler, A.; Antunovic, M.; Teruel Biosca, L.; Ferrer GG; Babic, S.; Urlic, I.; Ivankovic, M.... (2022). Osteogenic differentiation of human mesenchymal stem cells on substituted calcium phosphate/chitosan composite scaffold. Carbohydrate Polymers. 277:1-16. https://doi.org/10.1016/j.carbpol.2021.118883

Carbohydrate Polymers

Osteogenic differentiation of human mesenchymal stem cells on substituted calcium phosphate/chitosan composite scaffold

--Manuscript Draft--

Manuscript Number:	
Article Type:	Research Paper
Keywords:	chitosan; hydroxyapatite; osteogenic differentiation; perfusion-bioreactor; scaffolds; ionic substitution
Corresponding Author:	Antonia Ressler, mag. ing. cheming. Faculty of chemical engineering and technology Zagreb, CROATIA
First Author:	Antonia Ressler, Dr.
Order of Authors:	Antonia Ressler, Dr.
	Maja Antunović
	Laura Teruel-Biosca
	Gloria Gallego Ferrer
	Slaven Babić
	Inga Urlić
	Marica Ivanković
	Hrvoje Ivanković
Abstract:	In biomaterials for bone tissue regeneration, ionic substitutions are a promising strategy to enhance the biological performance of calcium phosphates and composite materials. However, systematic studies have not been found on multi-substituted organic/inorganic scaffolds. In this work, highly porous composite scaffolds based on calcium phosphates substituted with Sr2+, Mg2+, Zn2+ and SeO32- ions, and biodegradable polymer chitosan have been prepared by freeze-gelation technique. Scaffolds were characterized by Fourier transform infrared spectroscopy, X-ray diffraction, scanning electron microscopy, pore size distribution and porosity measurements. In vitro enzymatic degradation of scaffolds was characterized by swelling and dry weight remaining ratio measurements, molecular weight and microstructure determination. Enhanced osteogenic potential of human mesenchymal stem cells (hMSC) seeded on scaffolds has been determined by histological, immunohistochemical and RT-qPCR analysis of cultured cells in static and dynamic (U-CUP bioreactor) conditions. This work demonstrates the influence and importance of ionic substitutions on the osteogenic differentiation of hMSCs.
Suggested Reviewers:	Adriana Bigi adriana.bigi@unibo.it
	Susmita Bose sbose@wsu.edu
	Vuk Uskoković uskokovi@chapman.edu

Your MS Word document "Cover letter_Ressler.docx" cannot be opened or processed. Please see the list of common problems and suggested resolutions below.

Common Problems When Creating a PDF from Microsoft Word Documents

When you open your document in MS Word, an alert may appear. This message may relate to margins or document size. You will need to find the piece of your Word document that is causing the problem. Selectively remove various pieces of the file, saving the modified file with a temporary file name. Then try to open the modified file. Repeat this process until the alert no longer appears when you open the document.

Embedded Macros

Your submission file should not contain macros. If it does, an alert may appear when you open your document (this alert prevents EM from automatically converting your Word document into the PDF that Editors and Reviewers will use). You must remove these macros from your Word document.

Read-Only and Password-Protected Files

EM cannot process read-only or password-protected submission files. If your file is read-only or password-protected and you receive an error, please disable the document protection, save, and re-submit the file.

Corrupted Tables

Your document may contain a table that cannot be rendered correctly. This will be indicated by an alert. Correct the content of the table causing the problem so that the alert no longer appears.

Older MS Word files

EM supports files in MS Word 2000 and older versions. If you are using a more recent version of MS Word, try saving your Word document in the more recent format and resubmit to EM.

Other Problems

If you can get your Word document to open with no alert messages appearing and you have submitted it in a current MS Word format, and you still see an error message in your PDF file (where the Word document should be appearing), please contact the publication via the 'Contact Us' link on the EM Navigation Bar.' You will need to reformat your Word document and then re-submit it.

Osteogenic differentiation of human mesenchymal stem cells on substituted calcium phosphate/chitosan composite scaffold

Antonia Ressler[a]*, Maja Antunović[a], Laura Teruel-Biosca[b], Gloria Gallego Ferrer[b,c], Slaven Babić[d], Inga Urlić[e], Marica Ivanković[a], Hrvoje Ivanković[a]

[a] Faculty of Chemical Engineering and Technology, University of Zagreb, Marulićev trg 19, p.p.177, 10 000 Zagreb, Croatia

[b] Centre for Biomaterials and Tissue Engineering (CBIT), Universitat Politècnica de València, Camino de Vera s/n, 46022 Valencia, Spain

[c] Biomedical Research Networking Center on Bioengineering, Biomaterials and Nanomedicine (CIBER-BBN), 46022 Valencia, Spain

[d] UHC "Sestre milosrdnice", Department for Traumatology, Draškovićeva 19, 10 000 Zagreb, Croatia

[e] Department of Biology, Faculty of Science, University of Zagreb, Horvatovac 102a, Zagreb 10 000, Croatia

*Corresponding author: Antonia Ressler, Faculty of Chemical Engineering and Technology, University of Zagreb, Marulićev trg 19, p.p.177, 10 000 Zagreb Croatia, Tel: +385 01 4597 210, e-mail: aressler@fkit.hr

E-mail:

Antonia Ressler: aressler@fkit.hr

Maja Antunović: maja.antunovic2007@gmail.com

Laura Teruel-Biosca: lautebio@doctor.upv.es

Gloria Gallego Ferrer: ggallego@ter.upv.es

Inga Urlić: ingam@biol.pmf.hr

Slaven Babić: slaven.babic@gmail.com

Marica Ivanković: mivank@fkit.hr

Hrvoje Ivanković: hivan@fkit.hr

ABSTRACT

In biomaterials for bone tissue regeneration, ionic substitutions are a promising strategy to enhance the biological performance of calcium phosphates and composite materials. However, systematic studies have not been found on multi-substituted organic/inorganic scaffolds. In this work, highly porous composite scaffolds based on calcium phosphates substituted with Sr^{2+}, Mg^{2+}, Zn^{2+} and SeO_3^{2-} ions, and biodegradable polymer chitosan have been prepared by freeze-gelation technique. Scaffolds were characterized by Fourier transform infrared spectroscopy, X-ray diffraction, scanning electron microscopy, pore size distribution and porosity measurements. *In vitro* enzymatic degradation of scaffolds was characterized by swelling and dry weight remaining ratio measurements, molecular weight and microstructure determination. Enhanced osteogenic potential of human mesenchymal stem cells (hMSC) seeded on scaffolds has been determined by histological, immunohistochemical and RT-qPCR analysis of cultured cells in static and dynamic (U-CUP bioreactor) conditions. This work demonstrates the influence and importance of ionic substitutions on the osteogenic differentiation of hMSCs.

Keywords: chitosan, hydroxyapatite, osteogenic differentiation, perfusion-bioreactor, scaffolds, ionic substitution

1.Introduction

As life expectancy increases, so does the incidence of skeletal diseases resulting in requirements for new and more adequate regenerative materials for bone tissue (Aubin, 2008). Bone tissue is mainly composed of the calcium-deficient carbonated hydroxyapatite, representing 65-70% of the matrix and an organic phase composed of collagen (mainly of type I), glycoproteins, proteoglycans and sialoprotein, which comprises the remaining 25-30 % of the total matrix (Cardonnier, Sohier, Rosset, & Layrolle, 2011). From the biomimetic scaffold design perspective, achievement of molecular, structural and biological compatibility, while resembling as closely as possible the natural bone tissue should be achieved for a positive regenerative response. The integration of multiple stimuli physical factors (topography, porosity, pore size, stiffness, phase composition) and biochemical cues (grow factors, trace elements, genes or proteins) is the way forward to the next generation of biomimetic bone scaffolds. (Fernandez-Yague et al., 2015; Boanini, Gazzano, & Bigi, 2010) Biomimetic scaffolds should not only be biocompatible, but also promote proliferation and differentiation of progenitor cells and provide structural support until the newly-formed tissue has sufficient stiffness to stimulate the progression of the regeneration (Minardi et al., 2015).

Naturally derived polymers such as collagen, glycoaminoglycans, gelatin, chitosan, silk, fibrin, and elastin, have been widely used in a variety of tissue engineering applications. As these polymers show similarity with the extracellular matrix found in human physiology, they demonstrate appropriate biocompatibility for *in vivo* applications, but more importantly provide a range of ligands and peptides that facilitate cell-material communication to induce osteogenesis and in some cases reduce immunogeneicity. (Fernandez-Yague et al., 2015; Roseti, 2017; Deb, Deoghare, Borah, Barua, & Das Lala, 2018) Naturally derived polymer chitosan is widely used in bone tissue engineering due to minimal inflammatory body reaction, biocompatibility, biodegradability, and ability to provide a suitable environment for

cell growth. The $–NH_2$ groups, present in the chitosan polymer chain, are able to induce osteoblast differentiation. (Cardonnier et al., 2011; Muzzarelli, 2011) However, chitosan scaffolds are someway limited in inducing osteogenic differentiation of stem cells and usually need the combination with calcium phosphate (CaP) particles, tipically hydroxyapatite (HAp), to mimic the organic/inorganic nature of the bone (Venkatesan & Kim, 2010).

Recent trends have been focused on using pharmacologics and biologics to improve the osteogenic properties of synthetic organic and inorganic biomaterials. However, using growth factors is often related to ectopic or unwanted bone formation, and new trends look for biomimetic approaches based on trace elements naturaly present in the mineral phase of bone (Bose, Fielding, Tarafder, Bandyopadhyay, 2013). The high stability and flexibility of hydroxyapatite (HAp) structure allow a great variety of cationic and anionic substitutions. Ions, such as Sr^{2+}, CO_3^{2-}, Zn^{2+}, Mg^{2+}, Na^{+}, etc., which are present in biological apatites (Boanini et al., 2010) have been found to play a vital role in stem cells proliferation and differentiation, formation, growth and mineralization of extracellular matrix (ECM) (Bose et al., 2013).

Considering all mentioned above, biomimetic multi-substituted CaPs were used as inorganic phases within biopolymer chitosan to obtain highly porous scaffolds. Synergic effect of substituted ions in CaPs and biomimetic composite scaffold can have significant effect on differentiation of stem cells and bone regeneration. In our previous studies (Ressler et al., 2020a; Ressler, Antunović, Cvetnić, Ivanković & Ivanković, 2021; Ressler, 2020) individual and multiple ion substituted CaPs with various levels of Sr^{2+}, Zn^{2+}, Mg^{2+} and SeO_3^{2-} ion substitution have been prepared by wet precipitation method. Also, previous studies of our research group have proved non-cytotoxic and osteogenic properties of chitosan-unsubstituted hydroxyapatite scaffolds (Rogina et al., 2017, Ressler et al., 2018). Composite scaffolds with hydroxyapatite fraction of 30% (w/w) showed the strongest osteoinduction of mouse MC3T3-

E1 preosteoblasts and human mesenchymal stem cells (Rogina et al., 2017). The aim of this work was to study the effect of multiple ionic substitutions of Sr^{2+}, Zn^{2+}, Mg^{2+} and SeO_3^{2-} in CaPs on the osteogenic potential of chitosan-CaP scaffolds. The highly porous composite scaffolds, with 30 wt% of multi-substituted CaPs, were prepared by the freeze-gelation method and characterized. An extensive biological characterization in static and dynamic conditions has been performed, using human mesenchymal stem cells (hMSC). To the best of our knowledge, there are no data in literature regarding the effect of the studied multiple ionic substitutions in CaPs on the osteogenic potential of chitosan-CaP scaffolds.

2. Materials and methods

2.1. Preparation of composite scaffolds

The appropriate amount of chitosan was added to 0.40 wt% acetic acid solution to obtain 1.2 wt% chitosan solution at ambient temperature. The CaPs substituted with various trace elements (Sr^{2+}, Mg^{2+}, Zn^{2+} and SeO_3^{2-}) and precipitated from biogenic source (cuttlefish bone), were previously prepared in our studies (Ressler 2020, Ressler et al., 2021a, Ressler et al., 2021) and used to obtain composite scaffolds. Nominal composition and labels of prepared CaPs are given in Table 1. The appropriate amounts of each CaP, alone or in a mixture, were added to obtain 30 wt% of CaP in composite scaffold , based on the previous study (Rogina, Rico, Gallego Ferrer, Ivanković, Ivanković, 2014). The mass fraction of each CaP in the CaPs mixtures was the same (25 wt.%). The composite scaffolds are labeled as shown in Table 2. The chitosan/CaP suspensions were cooled to 4 °C, set in moulds, frozen, and kept at –30 °C for 8 h. Further, frozen samples were immersed into the neutralisation medium of 1 M NaOH/ethanol at –30 °C for 24 h to induce gelation of chitosan. The samples were rinsed in ethanol (96 wt%) at –30 °C for 24 h, washed with distilled water, frozen, and lyophilized.

Table 1. Nominal composition and labels of prepared CaP samples substituted with Sr^{2+}, Zn^{2+}, Mg^{2+} and SeO_3^{2-} ions (mol %) used as inorganic phase in composite scaffolds.

	Sample	Sr/(Ca+Sr) (mol %)	Zn/(Ca+Zn) (mol %)	Mg/(Ca+Mg) (mol %)	Se/(P+Se) (mol %)
Synthetic source	**CaP**	0	0	0	0
Biomimetic source (cuttlefish bone)	**CaP_0**	0	0	0	0
	1_Sr_CaP	1	0	0	0
	5_Sr_CaP	5	0	0	0
	1_Zn_CaP	0	1	0	0
	5_Zn_CaP	0	5	0	0
	1_Mg_CaP	0	0	1	0
	5_Mg_CaP	0	0	5	0
	1_Se_CaP	0	0	0	1
	5_Se_CaP	0	0	0	5

Table 2. Labels and type of CaPs in the prepared composite scaffolds.

Precursor for CaP	CaP	Composite sample	Wt.% of CaP in composite	Wt.% of CaP in the CaP mixture
Synthetic	CaP	SC	30	100
Biogenic	CaP_0	SC_0	30	100
	1_Sr_CaP	SC_1Sr		100
	5_Sr_CaP	SC_5Sr		100
	1_Zn_CaP	SC_1Zn		100
	5_Zn_CaP	SC_5Zn		100
	5_Zn_CaP	SC_1Mg		100
	1_Mg_CaP	SC_5Mg		100
	1_Se_CaP	SC_1Se		100
	5_Se_CaP	SC_5Se		100
				100
	1_Sr_CaP	SC_1MIX		25
	1_Zn_CaP			25
	1_Mg_CaP			25
	1_Se_CaP			25
	5_Sr_CaP	SC_5MIX		25
	5_Zn_CaP			25
	5_Mg_CaP			25
	5_Se_CaP			25

2.2. Scaffolds characterization

The Fourier transform infrared spectra (FTIR) of composite scaffolds were recorded by attenuated total reflectance (ATR) spectrometer for solids with a diamond crystal (Bruker Vertex 70) at 20 °C over the spectral range of 4,000 – 400 cm^{-1}, with 32 scans and 4 cm^{-1} of resolution.

Mineralogical composition of composite scaffolds was determined by X-ray diffraction analysis (XRD) using a Shimadzu XRD-6000 diffractometer with Cu Ka radiation operated at 40 kV and 30 mA, in the range of $3° < 2\Theta < 60°$ at a scan speed of 0.2°/2s. Indentification of crystal phases was done by International Centre for Diffraction Data (ICDD) card catalogue.

The morphology of composite scaffolds was imaged by the scanning electron microscope TESCAN Vega3SEM Easyprobe (SEM) at electron beam energy of 10 keV. Previously to imaging, samples were sputter coated with gold and palladium for 120 s. Obtained SEM images and ImageJ software were used to determine the diameter of 200 pores of obtained composite scaffolds. The results of pore size distribution are shown as pore density (%) of each pore range in relation to the total number of measured pores.

The porosity of the scaffolds was determined by Archimedes' principle, immersing each composite scaffold in ethanol at room temperature (T = 22.2 ± 0.3 °C) as previously described in our research (Ressler et al., 2020b, Morales-Román et al., 2019). Scaffolds porosity (%) is defined as the volume fraction of pores within the scaffold; so it was calculated as the volume of pores (V_p) devided by the total volume of the scaffold (V_{SC}) composed of pores and composite (V_c), Eq. (1):

$$Porosity\ (\%) = \frac{V_p}{V_{sc}} \square\ 100 = \frac{V_p}{V_p + V_c} \square 100 \quad (1)$$

The previously prepared scaffolds were cut with biopsy puncher into cylindrical shape pieces of 6 mm diameter ($\varnothing$) with uniform thickness (h) of ~1 mm. The dry samples (n = 5) were initially weighted (m_d). The volume of the pores was calculated by filling them with ethanol (ρ = 0.789 g/mL). After immersion in ethanol under vacuum atmosphere, excess liquid was removed and samples were weighted again (m_e). The density of cylindrically-

shaped scaffold is calculated according to the Eq. (2), the volume of the scaffold (V_{SC}) according to Eg. (3) and the pore volume was calculated according to Eq. (4):

$$\rho_{SC} = \frac{m_d}{\pi \times (Ø/2)^2 \times h} \quad (2)$$

$$V_{SC} = \frac{m_d}{\rho_{SC}} \quad (3)$$

$$V_p = \frac{m_e - m_d}{\rho_e} \quad (4)$$

2.3. In vitro enzymatic degradation

The degradation behaviour of obtained composite scaffolds (SC, SC_0, SC_1MIX, SC_5MIX) was studied at two different concentrations of lysozyme (1.5 μg/mL, corresponding to an activity of 164 U/mL, and 150 μg/mL, corresponding to an activity of 16 400 U/mL) under static physiological conditions in phosphate buffer saline solution (PBS). The degradation behaviour of composite scaffolds in the PBS solution without lysozyme was used as a control. Composite scaffolds (n = 5, Ø = 6 mm, h ~ 1 mm) were incubated in 5 mL of PBS containing lysozyme at 37 °C during 28 days. Freshly prepared degradation medium was changed every third day to maintain the activity of lysozyme and to mimic physiological conditions *in vivo* (Porstmann et al., 1989). At defined time points, the degradation medium was removed in order to determine the mass of swollen samples (m_s). Then, samples were lyophilised (m_d) and the swelling ratio was calculated according to Eq. (5):

$$Swelling\ ratio(\%) = \frac{m_s - m_d}{m_d} \times 100 \quad (5)$$

The degradation of scaffolds was determined as the ratio of remaining hydrogel weight (m_d)

and initial weight of the sample (m_{d0}) before enzymatic degradation Eq. (6).

$$Dry\ weight\ remaining\ ratio(\%) = \frac{m_d}{m_{d0}} \times 100 \quad (6)$$

The influence of degradation medium on scaffolds' microstructure was analysed by SEM after 28 days of degradation. Dried degraded samples were coated with a plasma of gold and palladium for 120 s. The microscopic imaging was carried out by the electron microscope TESCAN Vega3SEM Easyprobe at electron beam energy of 15 keV.

2.4. Gel permeation cromatography

The molecular weight distribution of chitosan before and after enzymatic degradation was analysed by Gel Permeation Chromatography (GPC), at 35 °C, with a Waters Breeze GPC system and a 1525 Binary HPLC pump (Waters Corporation, Milford, MA) equipped with a 2414 refractive index detector and four serial Ultrahydrogel columns of water (7.8 mm ID X 30 cm) connected in series (1,000, 500, 150 and 200) (Sanmartín-Masiá, Poveda-Reyes and Gallego Ferrer, 2017). The degraded composite samples were dissolved in acetic buffer (CH_3COOH 0.5 M/CH_3COONa 0.2 M, pH = 4.5) at a concentration of 1 mg/mL. This buffer was also used as the eluent phase at a flow rate of 0.5 mL/min (Gámiz-González, 2017). A volume of 2 mL of sample solution was prepared and left dissolve at room temperature in glass vials (covered with aluminun foils to protect the polymer from UV light). They were kept under agitation for 72 h to properly dissolve. Then, the samples were filtered and injected in the equipment by using 100 µL of sample per injection. A minimum of 3 replicates per sample were measured. The calibration curve was prepared by using monodisperse polyethylene glycol (PEG) standards of known molar mass at peak, supplied by Waters.

Mark-Houwink-Sakurada equation and Mark-Houwink parameters for PEG and chitosan were used to calculate the molecular weight of chitosan from the value obtained in the calibration curve.

2.5. Biological evaluation

2.5.1. Human Mesenchymal Stem Cells Isolation and Expansion

The bone marrow sample was collected during the surgery at the University Hospital of Traumatology in Zagreb (Croatia) with the patient's consent and approval of the Ethics Committee. The hMSCs were isolated using previously described method by Matić and associates (Matić et al., 2016). Briefly, bone marrow aspirates were added to Dulbecco's modified Eagle medium (DMEM) – low glucose containing 10% fetal bovine serum (FBS, Gibco), 100 U/mL penicillin and 100 g/mL streptomycin (Lonza). The suspension was centrifuged and pelleted cells were washed twice in PBS (Gibco). Resuspended cells were strained through a cell strainer (100 μm, BD Biosciences) to remove mineral bone residuals and centrifuged again. Cells were plated in 100 mm Petri dishes (Sarstedt) at a density of $1 \cdot 10^8$ in proliferation medium DMEM-low glucose, supplemented with 10% FBS, 100 U/mL penicillin and 100 μg/mL streptomycin and 10 ng/mL human fibroblast growth factor 2 (FGF2, Gibco), and kept in a humidified incubator at 37 °C with a 5% CO_2. After 24 h the non-adherent cells were removed, and the attached cells were grown. After 80% confluence, hMSCs were detached with 0.25% trypsin/EDTA (Sigma-Aldrich) and then subcultured for expansion (passage 1–5). The proliferation medium was changed every 2–3 days.

2.5.2. Static 3D cell culture of Human Mesenchymal Stem Cells

Composite scaffolds (SC, SC_0, SC_1MIX and SC_5MIX) were cut into cylindrical pieces of 6 mm diameter and ~1 mm height, sterilised in 96 % ethanol for 24 h. After sterilisation, scaffolds were washed 3 times with PBS (Gibco – Thermo Fisher Scientific) and left in proliferation medium DMEM-low glucose, supplemented with 10% FBS, 100 U/mL

penicillin and 100 μg/mL streptomycin and 10 ng/mL human fibroblast growth factor 2 (FGF2, Gibco) for 24 h at 4 °C. The following day, scaffolds were transported into polystyrene 96-well plates with a hydrophobic surface (Corning – Sigma Aldrich). The hMSCs were seeded on each scaffold in a concentration $2 \cdot 10^5$ cells/200 μL of medium per well. The cell suspension was added on each scaffold and incubated for 30 min in the incubator to allow cell attachment and migration inside the scaffold. Following the incubation period, the medium was added to a final volume of 200 μL per well. Each experiment was performed in triplicate and blanks were included as well. The cells were kept in a 5 % CO_2 humidified atmosphere at 37 °C for 14 and 21 days, respectively. After 14 and 21 days of cell culture, the scaffolds were put in TRIzol and kept at -80°C until analyzed.

2.5.3. Dynamic 3D cell culture of Human Mesenchymal Stem Cells in Perfusion Bioreactor

A perfusion bioreactor (U-CUP Cellec Biotek) was used to better simulate *in vivo* conditions by *in vitro* 3D culture of bone promoting scaffolds. Two samples of each scaffold (SC and SC_5MIX), with a diameter of 8 mm and a height of 1 mm, were inserted into the bioreactor for cell seeding with a cell suspension of $2 \cdot 10^6$ cells/scaffold in a total volume of 10 mL of proliferation medium per bioreactor. The closed bioreactor chamber was placed in the incubator at 37 °C and 5% CO_2 for 48 h and the flow rate for the perfusion of cells was settled at 1.7 mL/min. Following the 48 h-period, the proliferation medium was replaced by osteogenic induction medium containing: Minimum Essential Medium-Alpha Eagle (α-MEM, Lonza), 10% FBS, 1% penicillin/streptomycin, 50 μg/mL ascorbic acid (Sigma-Aldrich), 4 mmol/L *β*-glycerophosphate (Sigma-Aldrich) and 1×10^7 mol/L dexamethasone (Sigma-Aldrich). The cell culture flow rate (perfusion speed) was set at 0.6 mL/min during the culture and the bioreactor was placed in the incubator at 37 °C and 5% CO_2. The osteogenic medium was exchanged every 2–3 days according to the manufacturer's instructions (Cellec Biotech). After 21 days of cell culture, scaffolds were removed from the bioreactor and analyzed.

2.5.4 Gene expression analysis by qRT-PCR

The expression of genes related to osteogenesis, including alkaline phosphatase (ALP), bone sialoprotein (BSP) and dentin matrix protein 1 (DMP1) were analyzed by quantitative reverse transcription polymerase chain reaction (qRT-PCR). The qRT-PCR was performed to evaluate the expression levels of genes of cells cultured on scaffolds (SC, SC_0, SC_1MIX, SC_5MIX) after 14 and 21 days. The primer sequences used for PCR amplification are listed in Table 3.

Table 3. Human primer sequences used for determination of gene expression levels by reverse transcription-polymerase chain reaction analysis.

Primers	**5'-**	**Sequences**	**Annealing temperature (°C)**
ALP	forward	CTGTTTACATTTGGATAC	57.4
	reverse	ATGGAGACATTCTCGTTC	61.6
BSP	forward	GGAGACTTCAAATGAAGGAG	57.9
	reverse	CAGAAAGTGTGGTATTCTCAG	56.4
DMP1	forward	CAACTATGAAGATCAGCATCC	58.8
	reverse	CTTCCATTCTTCAGAATCCTC	59.3

Total cellular RNA was isolated using TRIzol reagent (Invitrogen Life Technologies), according to the manufacturer's instructions. Briefly, samples were washed with cold PBS and homogenized in 1 mL of TRIzol (Thermo Fisher) using a mixer mill (Retsch) for 3 min at 30 Hz, followed by 200 µL of chloroform addition and centrifugation for 15 min at 12,000 × G and 4 °C. The supernatant was separated, isopropanol and 0.5 µL of glycogen were added, after which the RNA was precipitated by centrifugation for 10 min at 15,000 × G and 4 ° C. The supernatant was separated and 1 mL of 75% ethanol was added to the RNA pellet, and the samples were centrifuged for 5 min at 15,000 × G and 4 ° C. The supernatant was separated and the RNA pellet was air dried for ~10 min and dissolved in 30 µL of water

treated with diethyl pyrocarbonate (DEPC). RNA concentration and purity were determined using the Nanodrop 2000 (Thermo Scientific, USA). To remove residual genomic DNA from isolated RNA, the prepared RNA suspension was treated with deoxyribonuclease I (Dnaze I, Invitrogen Life Technologies). Enzymatic removal of residual DNA from the sample was performed using a commercial purification kit (Thermo Scientific, USA) according to the manufacturer's protocol. A mixture for DNA degradation in a total volume of 20 µL was prepared. The reaction mixture contained Dnase, 10 × buffer, DEPC-treated water and a sample of isolated RNA of known concentration. The final mass of RNA in the reaction was 0.5 µg. The reaction mixture was homogenized and DNA digestion was performed by incubating the mixture for 60 minutes at 37 °C. Then 1.5 µL of ethylenediaminetetraacetic acid (EDTA) solution was added to the samples, and Dnasa I was inactivated by incubating the samples for 10 minutes at 65 ° C. Dnase I treated RNA was inversely transcribed into complementary DNA (cDNA) using a commercial High-Capacity cDNA Reverse Transcription Kit (Applied Biosystems) according to the manufacturer's protocol. Then 1.5 mL of the reaction mixture was prepared and mixed with each sample (10 µL RNA). The resulting mixture was homogenized and incubated according to the protocol. Samples were diluted with 5 µL of ultrapure water and stored at -20 ° C for further analysis.

Relative gene expression was determined by RT-qPCR using the 7500 Fast Real-Time PCR System (Applied Biosystems), commercially available primers (Sigma-Aldrich) and Power SYBR Green Mastermix (Applied Biosystems) were used. Each reaction consisted of a duplicate in 96-well plates (ABI PRISM Optical 96-Well Plate, Applied Biosystems). The PCR reaction was conducted under the following conditions: 10 min at 95 °C for 1 cycle, 15 s at 95 °C, and 1 min at 58 °C for 40 cycles. The expression levels of osteogenic genes were normalized to *18SRNA* as a housekeeping gene and calculated using the $^{\Delta\Delta}$Ct method.

2.5.5. Histological Analysis

After removing from static and dynamic cell culture, cultured samples after 14 and 21 days were rinsed in PBS, fixed in 4% paraformaldehyde, embedded in paraffin and cross-sectioned (5 μm thick) and stained with hematoxyline-eosin (H&E). All sections were deparaffinised using xylene, and rehydrated through a series of ethanol washes prior to staining.

Detection of phosphate deposits on composite scaffolds was determined using von Kossa staining. Samples were washed with distilled water and incubated in a 5% $AgNO_3$ solution (Sigma-Aldrich) under UVB light (UVB Crosslinker, Cleaver Scientific) for 3 min. Further, samples were washed with distilled water and 2% $Na_2S_2O_3$ (Sigma-Aldrich) to remove unreacted $AgNO_3$. All slides were dehydrated and mounted with a resinous medium (Biognost). Slides were observed under a microscope Olympus BX51.

2.5.6. Immunohistochemical detection of collagen type I

Collagen type I (COLL I) was detected using EnVision Detection Systems Peroxidase/DAB, Rabbit/Mouse (Dako/Agilent, Santa Clara, CA, USA) and anti-collagen I (Abcam, Cambridge, UK), as previously described with slight modification (Rogina et al. 2017). Briefly, sections were deparaffinised and rehydrated. Nonspecific binding sites were blocked with 10% goat serum (Dako) in PBS for 60 min at room temperature. Sections were then incubated with primary antibody (anti-collagen I, Abcam, Cambridge, UK), diluted 1:400 with 1% goat serum in PBS, overnight at 4 °C. After washing, the signal was detected with EnVision Detection Systems Peroxidase/DAB, Rabbit/Mouse (Dako), according to the manufacturer instructions. Hematoxylin was used as a counterstain. Human bone was used as a positive control. Slides were observed under a microscope Olympus BX51.

2.6. Statistical Analysis

The swelling and dry weight remaining ratio masurements were performed in quintuplicate (n = 5), and RT-qPCR experiments were performed in duplicate (n = 2). All data were expressed as mean ± standard deviation. Statistical analysis was performed using a one-way

ANOVA test followed by a post-hoc test to evaluate the statistical significance between groups. A value of $p < 0.05$ was considered statistically significant.

3. Results

3.1. The composition identification and morphology of scaffolds

The characterization of prepared systems was performed by FTIR spectroscopy (Fig. 1A) and XRD mineralogical analysis (Fig. 1B). The FTIR spectra for all prepared composite scaffolds with different trace elements content, pure chitosan scaffold (CS) and hydroxyapatite powder (HAp) have been shown in the range 400–1750 cm^{-1}. At the wave numbers >1550 cm^{-1} significant bands for were not detected.

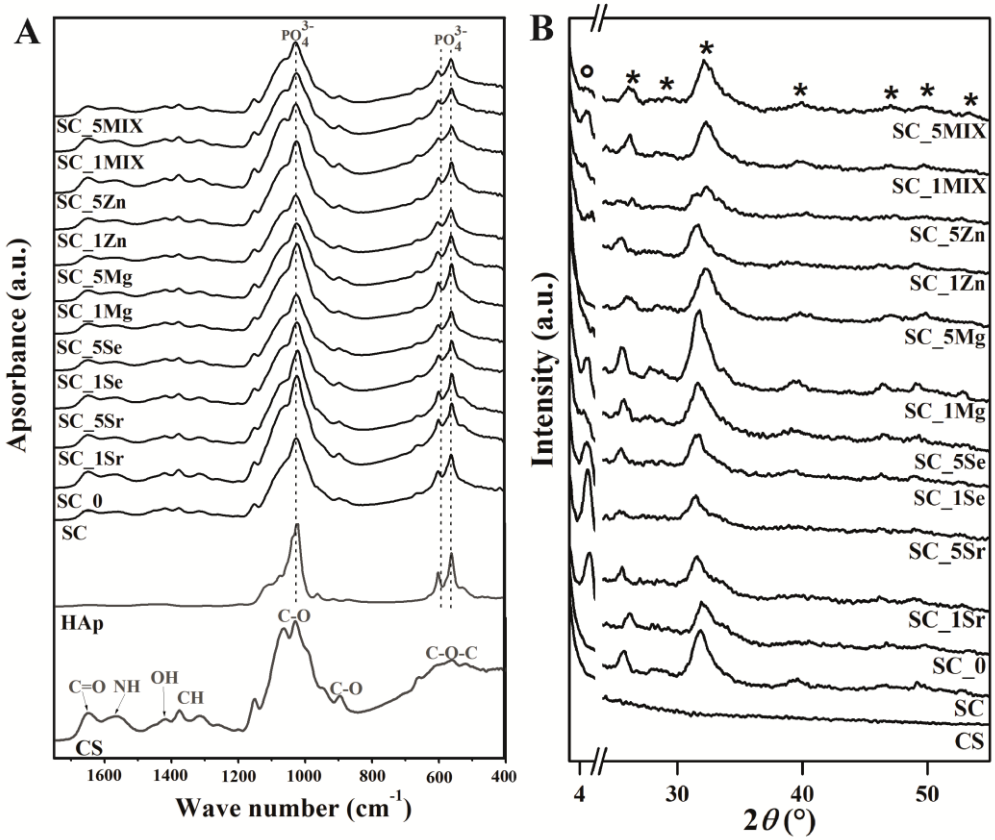

Figure 1. FTIR spectra (A) and XRD pattern (B) of prepared composite scaffolds with different substitution elements in CaP structure. Chitosan (CS) scaffold and pure

hydroxyapatite (HAp) were used as a control. Characteristic HAp (ICDD 9-432) diffraction maxima are depicted as (*) and OCP (ICDD 11-0293) as (°).

Absorption bands characteristic for chitosan are visible in all prepared scaffolds: at 1653 cm^{-1} corresponding to amid I (carbonyl band of amid), at 1567 cm^{-1} attributed to amid II (amino band of amid), 1422 cm^{-1} and 1324 cm^{-1} that correspond to the vibrations of OH and CH in the ring, 1378 cm^{-1} to CH_3 in amide group. Along with characteristic bands for the chitosan, typical bands for PO_4^{3-} groups in HAp structure were found at 565 cm^{-1} and 600 cm^{-1} that can be assigned to asymmetric bending vibrations of O–P–O, and at 1028 cm^{-1} attributed to the asymmetric stretching vibration of P–O.

The CaP powders substituted with Sr^{2+}, Mg^{2+}, Zn^{2+} and SeO_3^{2-}, obtained in our previous studies from biogenic source (cuttlefish bone), have been used as the inorganic phase in prepared composite scaffolds (Ressler et al., 2020a; Ressler et al., 2021; Ressler, 2020). The powder samples were mainly composed of calcium-deficient HAp, octacalcium phosphate (OCP, $Ca_8(HPO_4)_2(PO_4)_4 \cdot 5H_2O$) and amorphous calcium phosphate (ACP) phases.

The XRD analysis of composite scaffolds confirmed the presence of HAp in all prepared samples as a main mineralogical phase. Contrary to expectations, the diffraction patterns of SC_0, SC_1Sr, SC_5Sr, SC_5Se and SC_1MIX revealed the coexistence of HAp and OCP. A minor amount of OCP phase has been detected in SC_1Se, SC_5Zn and SC_MIX composite scaffolds. The calcium-deficient HAp, with a Ca/P ratio 1.50–1.67, is stable within pH range 6.5–9.5, while OCP, with a Ca/P ratio 1.33, is stable within pH range 5.5–7.0. The chitosan and CaP suspension has been frozen and neutralized in NaOH/EtOH solution for 8 hours. Even if the pH of the NaOH/EtOH solution is >10, the portion of the OCP stayed stable despite of being thermodynamically less stable at a high pH. There are several possible explanations for this outcome. The OCP phase might be stabilized by substituent ions in its

structure and/or the neutralization time is too short for the OCP to fully transform to a thermodynamically more stable phase, HAp. It has been determined that the OCP phase occurs as an unstable intermediate phase during precipitation of more stable CaPs in aqueous solutions. The central OCP inclusion determined in biological apatite and synthetic precipitated HAp confirms obtaining more stable phases by transformation from the firstly formed OCP phase as explained by Dorozkin (Dorozhkin, 2014).

The SEM analysis and ImageJ software were used to determine the microstructure and pore size distribution of prepared composite scaffolds SC, SC_0, SC_1MIX and SC_5MIX. Fig. 2 shows highly porous structures with interconnected pores. The CaPs particles are homogeneously dispersed in the chitosan matrix. The determined pore volume fraction was 74.3 ± 0.1 % in SC, 75.1 ± 0.2 % in SC_0, 75.3 ± 0.2 % SC_1MIX and 72.3 ± 0.2 % in SC_5MIX scaffold. The distribution of pore size (Fig. 2) revealed no significant difference between obtained samples. The pore size ranged from ~20 to ~350 μm in all obtained scaffolds. The composite scaffolds SC_1Sr, SC_5Sr, SC_1Se, SC_5Se, SC_1Zn, SC_5Zn, SC_1Mg and SC_5Mg have not revealed a difference in morphology compared to scaffolds SC, SC_0, SC_1MIX and SC_5MIX.

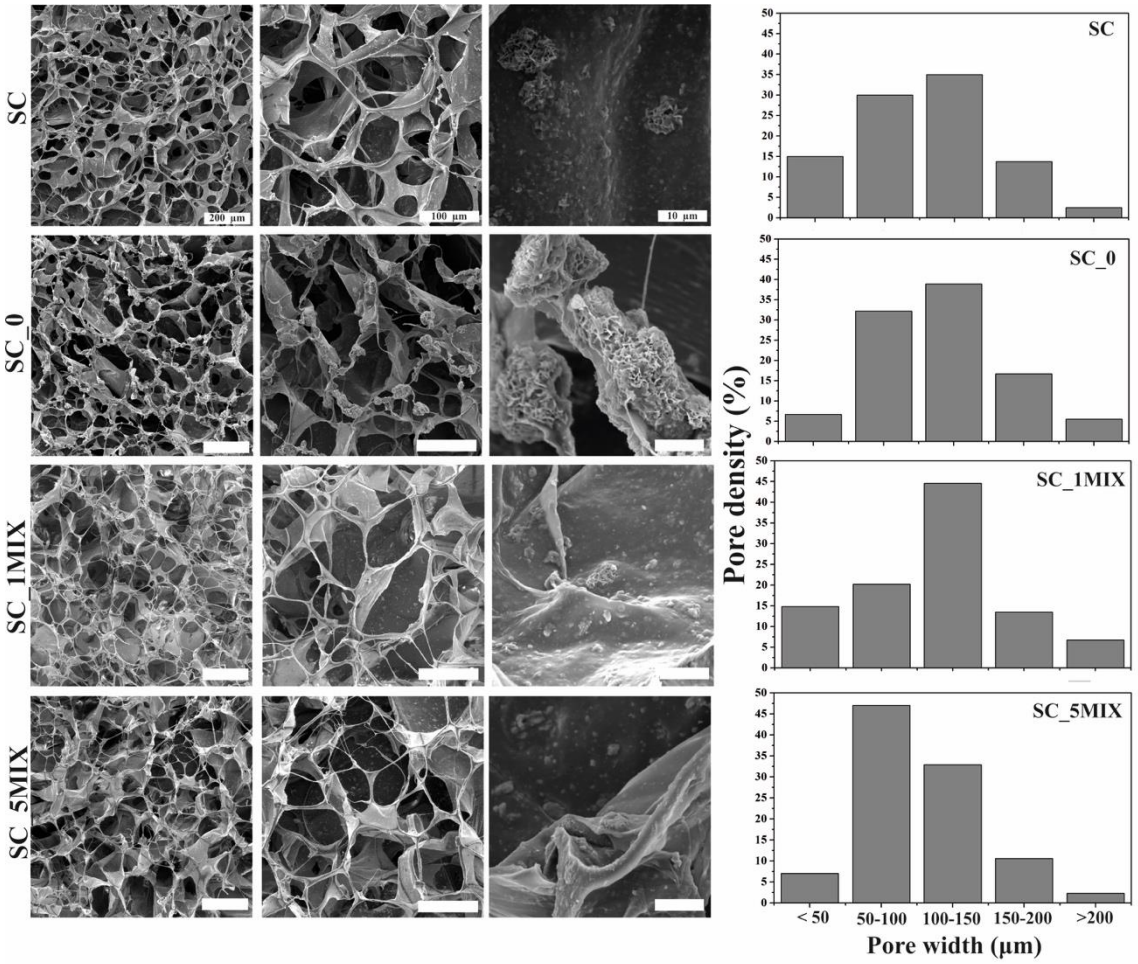

Figure 2. Microscopic imaging (left) and pore size distribution (right) of prepared composite scaffolds (SC, SC_0, SC_1MIX, SC_5MIX). Scale bar: 200, 100 and 10 µm.

3.2. In vitro degradation testing

Biodegradation of porous scaffolds is a complex process, where the degradation rate depends on various scaffold characterisitc as porosity, pore size, surface area, hydrophilicity, polymer structure, etc. The enzymatic hydrolytic degradation by lysozymes is the primary mechanism of chitosan degradation in the human body (Kalantari, Afifi, Jahangirian, Webster, 2019). The enzymatic degradation of SC, SC_0, SC_1MIX and SC_5MIX was studied at 37 °C as a function of time, for 28 days, by monitoring swelling behaviour, dry weight loss, weight average of molecular weight (M_w) and dispersity ($Đ_M$). To distinguish between dissolution

and enzymatic degradation, composite scaffolds were exposed to PBS solution without (0 μg/mL) lysozyme, and with (1.5 and 150 μg/mL) lysozyme, mimicking the *in vivo* physiological conditions. The concentration of lysozyme in human serum is in the range 0.95–2.45 μg/mL and can increase up to 1,000- fold in the extracellular matrix (Hou, Hu, Park, & Lee, 2012).

The results shown in Fig. 3A did not reveal a further increase of swelling ratio after initial water uptake at 0 day. There is no significant difference in swelling ratios with incubation time in degradation medium with 0, 1.5 and 150 μg/mL of lysozyme. As seen from Fig. 3B, at day 14 the dry weight remaining ratio of all incubated scaffolds decreases as lysozyme concentration increases. After 28 days of incubation, the dry weight remaining ratio in different lysozyme solutions significantly decreases for all analysed scaffolds. The changes in molecular weight were monitored by GPC measurements. As shown in Fig. 4A for SC_5MIX scaffold the weight average molecular weight (M_w) decreased during incubation time in all investigated scaffolds, and as expected, the degradation is the most pronounced in 150 μg/mL of lysozyme solution. In the PBS solution (without lysozyme) no significant change in molecular weight was observed after 14 days of incubation, but, significant change was observed after 28 days. In the solution with 1.5 μg/mL of lysozyme a significant decrease of M_w occur, from initial $M_{w0} \approx 180{,}000$ to 147,500 and 94,000, at day 14 and 28, respectively. In the solution with 150 μg/mL of lysozyme a significant decrease of M_w to 43,000 was observed after 14 days. Between days 14 and 28 no significant change of M_w was observed. The initial $Đ_M$ of 2.37, increased after 14 and 28 days, in 0 μg/mL of lysozyme solution to 2.74 and 2.97, respectively, in 1.5 μg/mL of lysozyme solution changed to 2.74 and 2.33, respectively, and in 150 μg/mL of lysozyme solution decrease to 1.79 and 1.90, respectively. The increase of $Đ_M$ after incubation indicates that degradation products remained in the matrice. The $Đ_M$ decrease after 28 days in 1.5 μg/mL of lysozyme solution and after 14 and

28 days in 150 μg/mL of lysozyme solution indicates the release of low molecular weight degradation products into surrounding media that is related to pronounced weight loss (Ren, Yi, Wang and Ma, 2005).

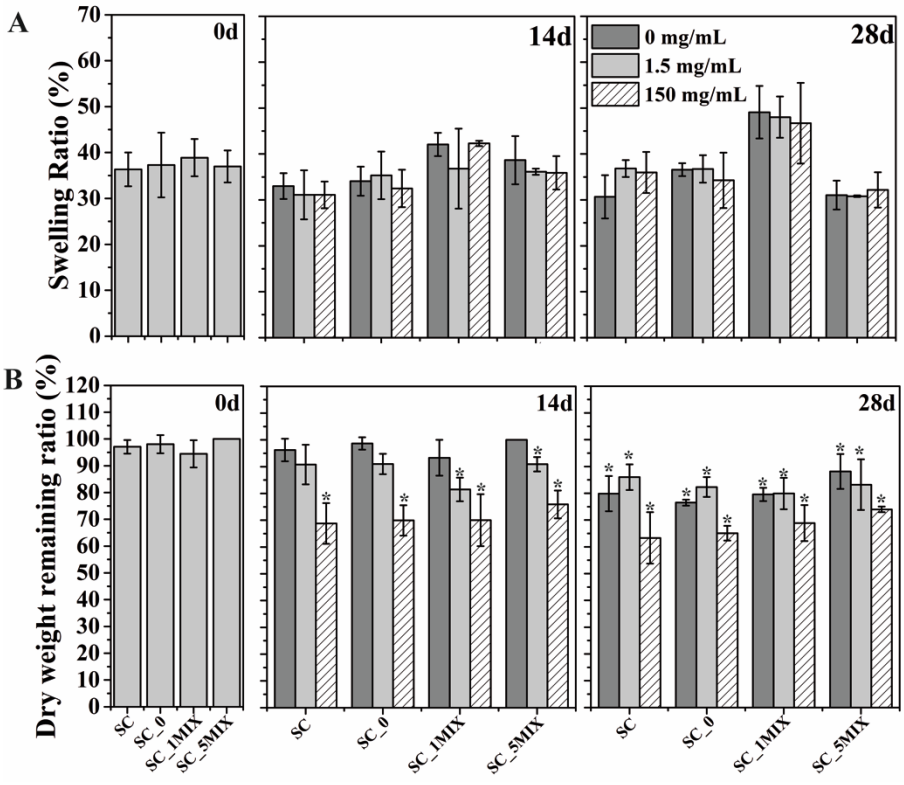

Figure 3. Swelling ratio (A) and dry weight remaining ratio (B) of composite scaffolds incubated in different degradation mediums at 37 °C as a function of time. Significant difference compared to scaffolds at 0 day: *($p < 0.05$).

The microstructures of the cross-section of SC, SC_0, SC_1MIX and SC_5MIX scaffolds shown in Fig. 4B after 28 days of incubation at 37 °C did not show significant difference to initial scaffolds (Fig. 2). Additionally, there is no a significant difference among the scaffolds incubated in different concentrations of lysozyme. The highly porous structure has been retained after 28 days of enzymatic degradation which is highly important for cell migration, diffusion of metabolic waste, oxygen and nutrients. The SEM micrographs confirmed highly

stable scaffold structure and uniform degradation through the entire scaffold volume despite a significant decrease of molecular weight in different degradation mediums.

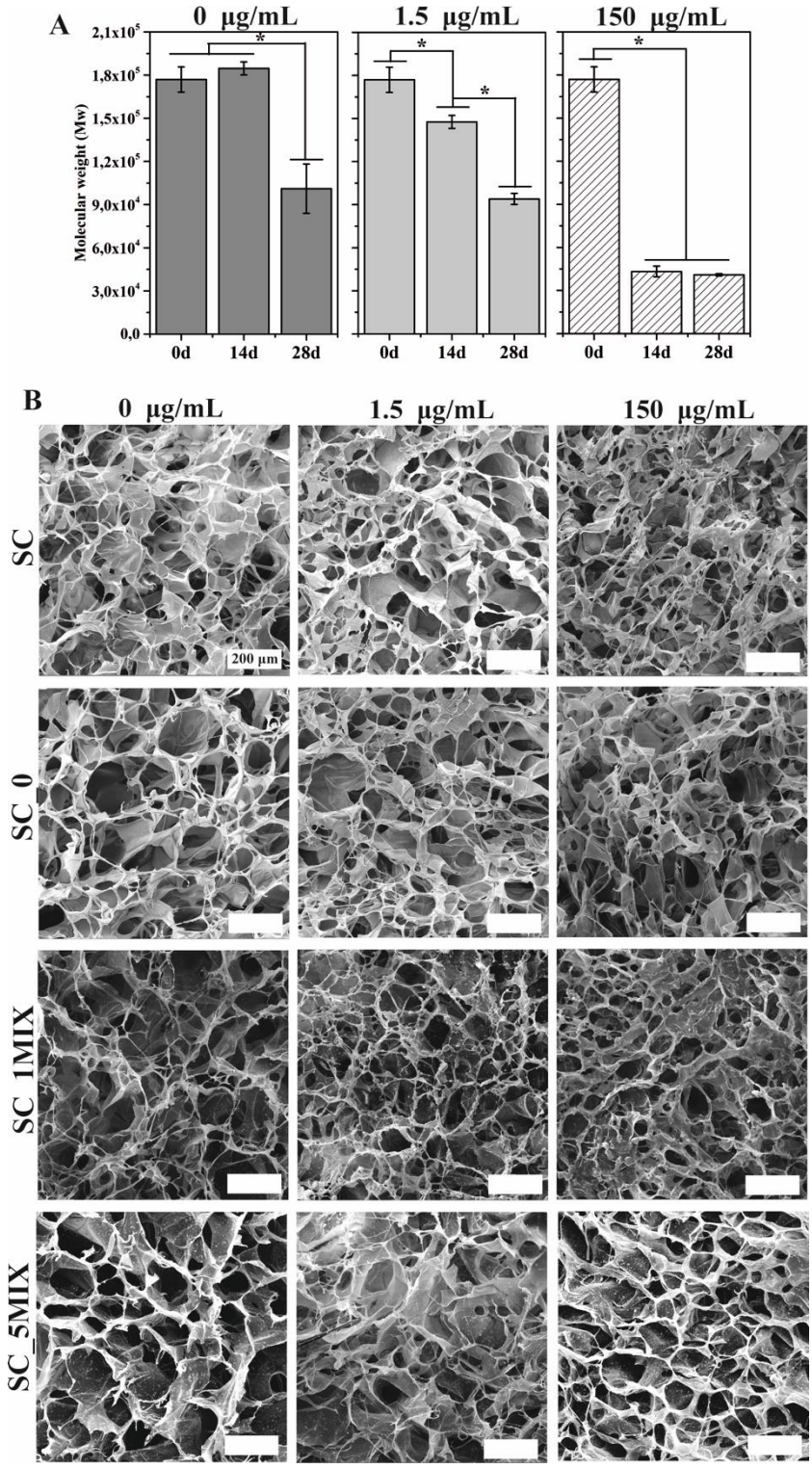

Figure 4. Weight average molecular weight of SC_5MIX scaffold (A) and SEM (B) micrographs of SC, SC_0, SC_1MIX and SC_5MIX scaffolds incubated in different

degradation media at 37 °C as a function of time. Significant difference compared to scaffolds at 0 day: *($p < 0.05$).

3.3. Biological characterization

3.3.4.Quantitative evaluation of osteogenic differentiation in static conditions

Relative expression of specific osteogenic markers (ALP, BSP and DMP1) on scaffolds SC, SC_0, SC_1MIX and SC_5MIX after 14 and 21 days of hMSCs culture in static conditions are shown in Fig. 5. The results were normalized to the SC sample.

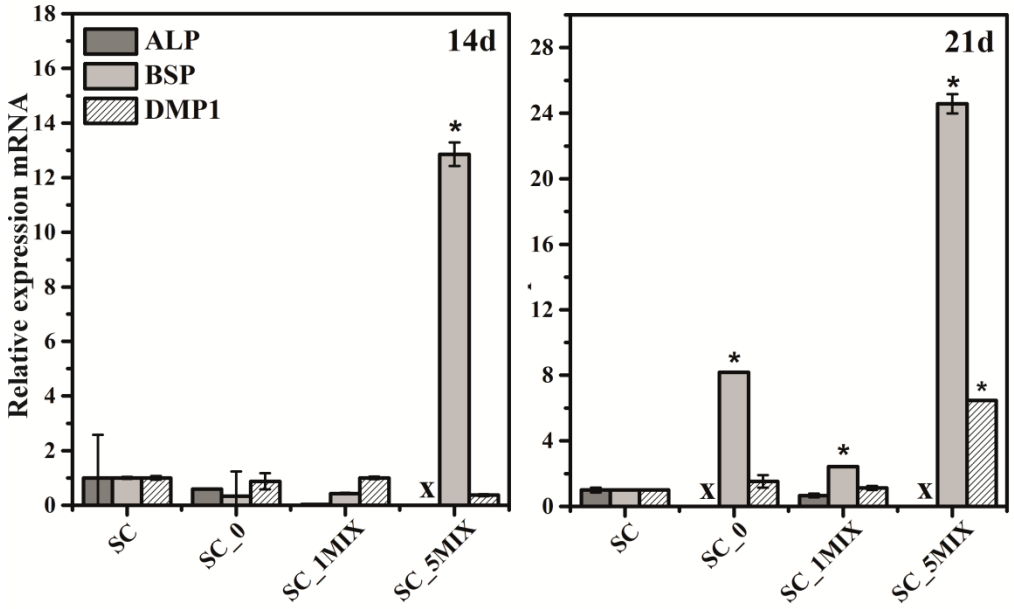

Figure 5. Relative expression of osteogenic markers (ALP, BSP and DMP1) after 14 and 21 days of static 3D culture. The relative gene expression was analyzed by the comparative cycle threshold method ($^{\Delta\Delta}$Ct) and the values were normalized to *18SRNA* expression. The significant difference compared to non-substituted scaffold (SC): * ($p < 0.05$).

ALP acts as an early indicator of cellular activity and differentiation and is the first functional gene expressed in the process of osteogenesis (Seibel, 2005; Golub & Boesze-Battaglia, 2007). The levels of ALP increase with the progress of osteoblastic differentiation, after

which expression of ALP decreases as mineralization progresses (Kulterer et al., 2007; Aubin, 2008). As seen from Fig. 5 after 14 and 21 days of cell culture low relative expression of ALP has been detected in analysed samples. The analysis did not reveal any significant difference in ALP expression among the composite samples. The BSP is a post-translationally modified acidic phosphoprotein expressed in mineralized tissues such as bone and dentin (Gordon et al., 2007). The potential to induce HAp nucleation and crystal formation indicate a potential role of the protein in the early stage of mineralization. In addition, BSP can bind to HAp through polyglutamic acid sequences and mediate cell attachment (Kirkham, & Cartmell, 2007). The BSP expression significantly increases in scaffolds SC_0 and SC_1MIX after 21 days of cell culture. Especially high BSP expression was determined for scaffold SC_5MIX after 14 and 21 days of cell culture.

The DMP1 protein expression, characteristic for mineralized tissues, preferentially is expressed by mature bone cells, osteocytes (Kalajzic et al., 2004). There were no significant differences in DMP1 protein expression among the analysed samples, expect a significantly higher expression of DMP1 after 21 days of cell culture in sample SC_5MIX.

3.3.5. Qualitative evaluation of scaffolds culltured in static conditions

The stem cells can differentiate into several cell lineages such as osteoblasts, chondrocytes, adipocytes, tenocytes and myoblasts with a low risk of transformation to tumor cells. The MSCs are often used in evaluation of the osteogenic potential of regenerative biomaterials. The stem cells can differentiate to functional matrix-synthesizing osteoblasts, while the process can be subdivided into three stages: (i) proliferation, (ii) formation of ECM and maturation, and (iii) ECM mineralization. During each stage, characteristic changes in gene expression can be detected. (Aubin, 2008) In this study, hMSCs were used to determine the osteogenic potential of prepared composite scaffolds (SC, SC_0, SC_1MIX and SC_5MIX)

after 21 days of cell culture. Scaffold without hMSC was used as negative control (Ctrl). Human bone was used as a positive control.

Histological analysis of scaffolds, determined by H&E (Fig. 6A) staining, points out a significant difference in the amount of newly formed tissue in the samples SC_1MIX and SC_5MIX compared to the scaffolds SC_0 and SC. The scaffold SC_0 with inorganic CaP phase obtained from a biogenic source showed a larger amount of formed tissue compared to scaffold SC, with un-substituted HAp phase obtained from synthetic precursors. The higher amount of formed tissue points the benefit of using biogenic sources in regenerative biomaterials. The analysed scaffolds only differ between each other in trace element composition and substitution level. From obtained results, it can be assumed that trace elements play a crucial role in stem cell differentiation to osteoblasts and bone regeneration.

Immunohistochemical analysis of scaffolds evaluated the production of type I collagen (COLL I) (Fig. 6B). The COLL I play a role in cell adhesion, proliferation and differentiation of osteoblast and is considered as an early indicator of osteoblastic differentiation (Kirkham & Cartmell, 2007; Kulterer et al., 2007). The positive staining of COLL I on all prepared scaffolds after 21 days of cell culture, indicate the early stages of osteogenesis. Along with homogenous expression through the scaffold, the intense localized staining was observed in the scaffold SC_5MIX.

Mineralized ECM in the analysed scaffolds was identified by von Kossa staining (Fig. 6C), where phosphate deposits are positively stained in brown and black. After 21 days of cell culture, higher intensity of brown (black) deposits in SC_0 and SC_5MIX indicate that mineralization of ECM occurred. Obtained results of differentiated cells after 21 days of cell culture were compared to the scaffold without seeded cells (negative Ctrl).

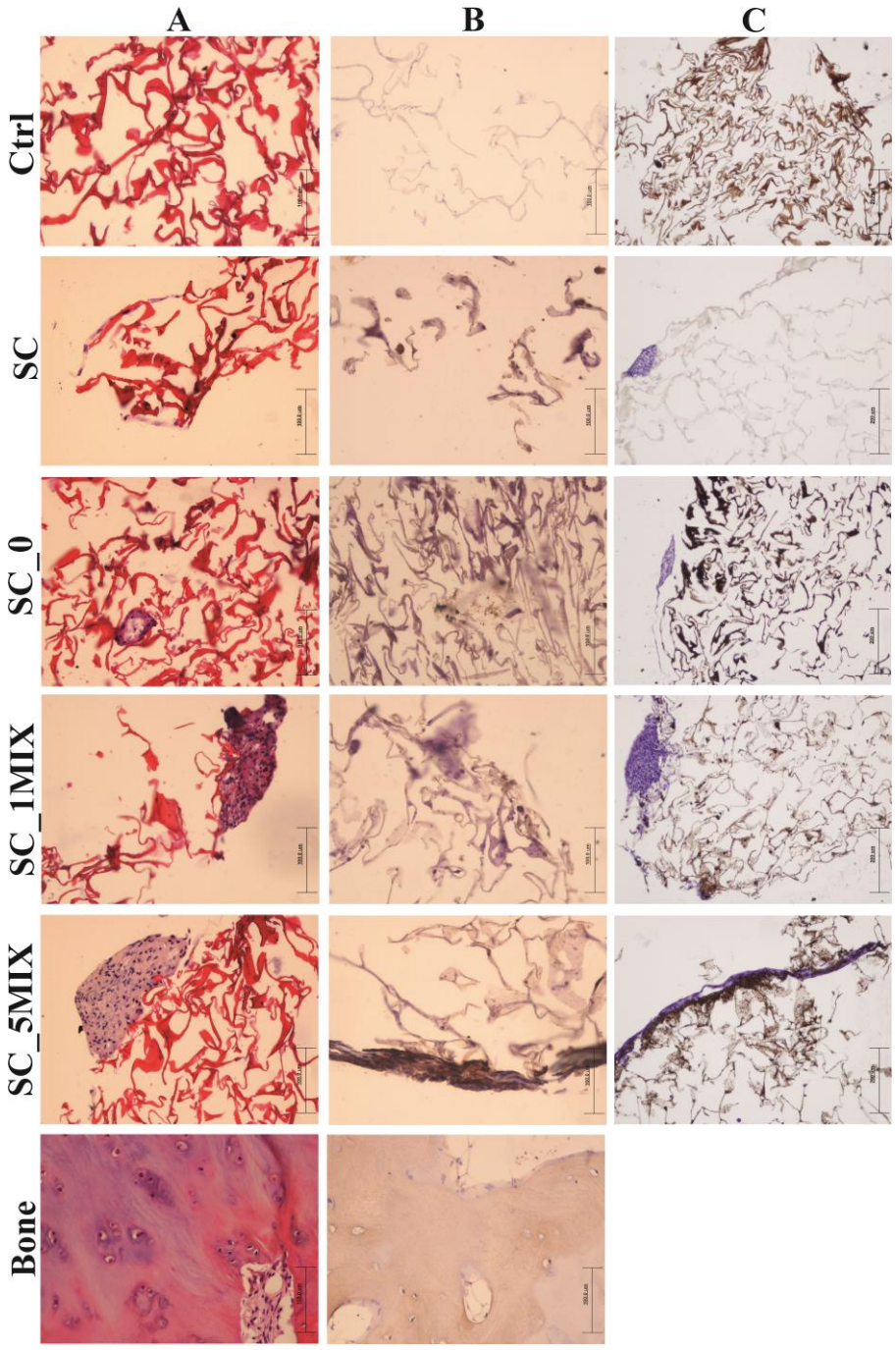

Figure 6. Detection of newly formed tissue, collagen I and mineralisation after 21 days of static 3D cell culture of hMSC on composite scaffold SC, SC_0, SC_1MIX, SC_5MIX. Hematoxylin-eosin (A) staining was used to observe newly-formed tissue, immunohistochemical (B) staining to observe collagen type I formation and von Kossa (C) staining for detection of mineralization (including hematoxylin counterstain). Scaffold

without hMSC was used as negative control (Ctrl). Human bone was used as a positive control. Scale bar: 100 (A and B) and 200 (C) μm.

3.3.6. Biological evaluation of scaffolds cultured in a perfusion bioreactor

As seen before, the scaffold SC_5MIX showed the highest formation of bone tissue, COLL I expression, phosphate deposition, and BSC and DMP1 protein expression. For this reason, biological evaluation of the scaffold SC_5MIX, cultured in dynamic conditions in perfusion bioreactor were performed.

In a bioreactor media flow obtained by perfusion forces provides physiochemical and biomechanical stimuli for new three-dimensional bony tissue growth. The osteogenic potential of the scaffold SC_5MIX was determined in the perfusion U-CUP bioreactor. H&E (Fig. 7A) staining was used to observe newly-formed tissue, COLL I (Fig. 7B) staining to observe collagen formation and von Kossa (Fig. 7C) staining for detection of mineralization (including hematoxylin counterstain). For comparison, scaffold SC was used, to determine the difference in newly-formed tissue, COLL I expression and phosphate deposition, while scaffold without hMSC was used as negative control (Ctrl).

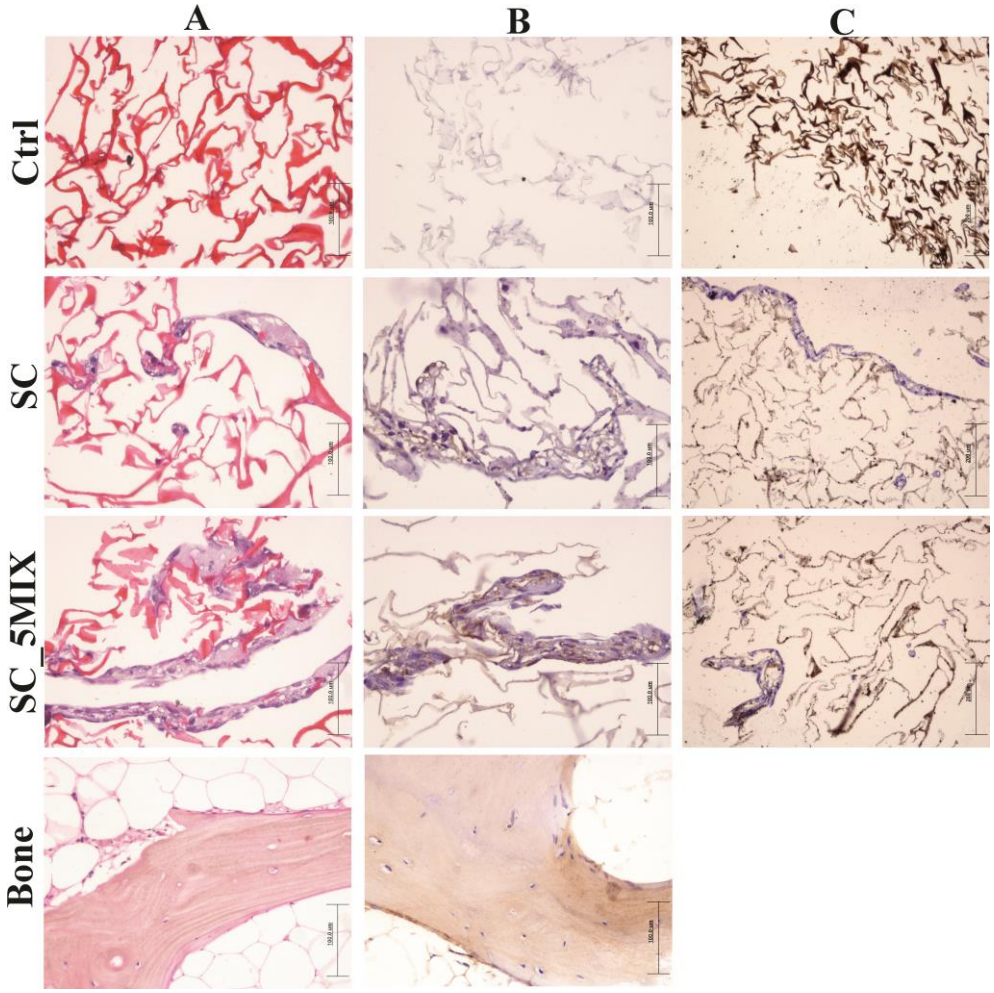

Figure 7. Detection of newly formed tissue, collagen I and mineralization after 21 days of dynamic 3D cell culture of hMSC on composite scaffold SC and SC_5MIX. Hematoxylin-eosin (A) staining was used to observe newly-formed tissue, immunohistochemical (B) staining to observe collagen type I formation and von Kossa (C) staining for detection of mineralization (including hematoxylin counterstain). Scaffold without hMSC was used as a negative control (Ctrl). Human bone was used as a positive control. Scale bar: 100 (A and B) and 200 (C) μm.

Histological analysis of scaffolds points out a difference in the amount of newly formed tissue in the scaffold SC_5MIX compared to scaffold SC. The newly-formed tissue is unifromly distributed through the volume of the scaffold SC_5MIX. It can be assumed that obtained scaffold`s composition is a suitable environment for hMSCs migration and growth after 21

days od cell culture. The positive staining to COLL I was determined in scaffolds SC_5MIX and SC after 21 days of cell culture, indicating the early stages of osteoinduction. Along with homogenous expression through the newly-formed tissue, the intense localized staining was determined in scaffold SC_5MIX. After 21 days of cell culture, brown (black) deposits in scaffolds SC_5MIX and SC indicate that mineralization of ECM occurred. Even the intensity of the color is lower than Ctrl, the deposition (black dots) can be seen after 21 days of cell culture.

4. Discussion

In our previous studies (Ressler et al., 2020a; Ressler et al., 2021; Ressler 2020), biomimetic triphasic CaPs powders substituted with Sr^{2+}, Mg^{2+}, Zn^{2+}, and SeO_3^{2-} ions were prepared by wet precipitation method, using biogenic source (cuttlefish bone) as a precursor of Ca^{2+} ions. The precipitated CaPs were composed of calcium-deficient carbonated HAp, OCP and ACP. Ion release study confirmed better resorbable properties of materials obtained from a biogenic source and substituted with ions, while phase transformation analysis at simulated physiological conditions confirmed the transformation of OCP and ACP to thermodynamically more stable phase, HAp, as it occurs in natural tissue. The culture of HEK 293 cells indicated noncytotoxicity of prepared CaP powders substituted with Sr^{2+}, Mg^{2+} and Zn^{2+} with emphasis on the cell proliferation during culture time. Additionally, the CaPs powders substituted with SeO_3^{2-} ions have shown selective anticancer properties at lower levels of substitution.

As a continuation of previous studies, highly porous composite scaffolds based on multi-substituted CaPs and biopolymer chitosan have been prepared and an extensive *in vitro* characterization using hMSC was performed, including enzymatic degradation during 28 days at simulated physiological conditions. It was hypothesized that substituted ions Sr^{2+}, Mg^{2+},

Zn^{2+}, and SeO_3^{2-} would provide a suitable environment for hMSCs differentiation with a positive influence on osteoinduction and newly-formed bone tissue.

Mineralogical phase composition is of high importance for suitable resorption and biological performance of prepared scaffolds. Recent studies are focused on obtaining two or three CaP phase systems to enhance the resorption properties of biomaterials. As explained in our previous studies, foreign ions influence the phase transformation of CaPs from amorphous to crystalline phases, resulting in the stabilization of metastable CaP phases. The attractive aspect of OCP as a bone substitute material has been studied by Suzuki et al. (Suzuki et al., 2006). It was demonstrated that the implantation of OCP markedly enhanced bone formation, osteoblastic cell proliferation and differentiation compared to the implantation of Ca-deficient HAp. (Suzuki et al., 2006) Obtained inorganic phase in prepared scaffolds consists of CaPs characterized by small dimensions, low crystallinity and non-stochiometric composition which are characteristics of natural apatite.

The pore diameter, pore size distribution, pore volume, pore shape and pore wall roughness are important factors for proper cell attachment, migration and tissue growth. The porosity of ~75 % in prepared composite scaffolds is in the range 50-90% suitable for the efficient bone regeneration process. Achieved interconnectivity between pores is essential for the diffusion of essential nutrients, oxygen and extracellular fluid in and out of the cellular matrix. Both macro and micro porosity play a vital role in the development of tissue inside the scaffold environment. Macroporosity, having a pore size of 100-400 μm, promotes osteogenesis by enhancing cell migration, cell-cell network formation, vascularization, nutrients supply, and metabolic waste diffusion. Microporosity, with a pore size < 20μm, is crucial for cell seeding and retention, capillaries growth, vascularization and cell-matrix interactions. (Fernandez-Yague et al., 2015; Deb et al., 2018) The achieved porosity and pore size requirements of the prepared scaffold should allow rapid and abundant vascularization network, essential to avoid

implanted-cell necrosis, formation of acellular regions and to allow new tissue formation (Cardonnier et al., 2011).

Swelling behaviour, structural stability and degradation rate are highly important in order to allow tissue formation to occur simultaneously with degradation. The scaffolds obtained from natural polymers often undergo rapid degradation, difficult to control, under physiological conditions. (Karageorgiou & Kaplan, 2005; Roseti et al., 2017) Chitosan has the ability to swell under physiological conditions giving a microenvironment similar to natural bone tissue suitable for cell attachment and growth. As explained in our previous research (Ressler et al., 2018), chitosan degrades *via* hydrolysis, where polymer network breaks into smaller chains, whereby the β-1-4 N-acetyl glucosamine units undergo chain scission mainly by lysozymes present in body fluid. Degradation products of chitosan are non-toxic, manily composed of glucosamine and saccharide, which can then be easily excreted from the body without interference with other organs (Kalantari et al., 2019). The obtained results show that prepared scaffolds, based on natural polymer chitosan, are highly stable during 28 days at physiological conditions, and in a much higher concentration of lysozyme, which is highly important for supporting newly formed bone tissue. The reason for this outcome could be the higher molecular weight of chitosan and deacetylation degree. Chitosan with a high DD tends to have a slower degradation rate due to closer chain packing and hydrogen bonding (Kalantari et al. 2019).

The MSCs are shown promising potential as a source of cell-based therapeutic strategies. These cells can differentiate into osteoblasts, chondrocytes, adipocytes, tenocytes and myoblasts and thus may be used in multiple types of cellular therapeutic strategies for regeneration of all tissues as bone, cartilage, fat, muscle, tendons and ligaments (Aubin, 2018; Kulterer et al., 2007). In bone tissue, the MSCs seem to migrate and attach to the scaffold surface *in vivo* from day one after implantation, depositing bone-related proteins and creating

a non-collagenous matrix layer on the implant surface that regulates cell adhesion. This matrix is an early-formed calcified afibrillar layer on the surface, involving poorly mineralized osteoid that is rich in calcium, phosphorus, osteopontin and BSP (Mavrogenis, Dimitriou, Parvizi, Babis, 2009).

The recent uses of growth factors have proven the advantage of manipulating synthetic materials to enhance the bone regenerative process. However, the safety and stability of growth factors have been questioned. In recent years, many studies have focused on the biomimetic approach and incorporation of trace elements, crucial for bone function, into synthetic materials (Bose et al., 2013). The CaPs used in this work are substituted with Sr^{2+}, Mg^{2+}, Zn^{2+}, and SeO_3^{2-} ions, along with Na-substitution as a result of using cuttlefish bone as a precursor of Ca^{2+} ions. The biocompatibility test of ion substituted CaPs has been obtained in our previous research, as the high intake of ions can have a negative side effect on cells. Further, the biocompatibility test of prepared composite scaffolds confirmed biocompatibility and the ability to promote cell proliferation. Significantly higher live cell (%) after 7 days of culture, compared to non-substituted scaffold SC, indicate a beneficial effect of substituted ions on cell proliferation (dana not shown).

Bonnelye et al. determined the dual mode of action of Sr^{2+} ions, where Sr^{2+} ions increased expression of osteoblastic markers ALP, BSP and osteocalcin while decreasing osteoclasts activity (Bonnelye, Chabadel, Salterl, Jurdic, 2008). A similar tendency was observed in *in vivo* studies of collagen-Sr-HAp scaffold developed by Yang et al. As explained, the calcium-sensing receptor (CaSR) is involved in the Sr-induced proliferation of the osteoblasts and the apoptosis of osteoclasts (Yang et al., 2011). Strontium activates the CaSR in osteoblasts, downstream signaling pathways, which promote osteoblast proliferation, differentiation, and survival, while at the same time cause osteoclast apoptosis resulting in a decrease of bone resorption. The CaSR simultaneously increases osteoprotegerin (OPG) production and

decreases receptor activator of nuclear factor kappa beta ligand (RANKL) expression. OPG is a protein that inhibits RANKL-induced osteoclastogenesis by operating as a decoy receptor for RANKL. The OPG/RANKL ratio, additionally controlled by Sr-introducing, can be a powerful regulator of bone resorption and osteoclastogenesis (Bose et al., 2013).

In natural bone tissue, along with calcium, magnesium is the second „messenger“ for regulating a wide variety of reactions involved in cell response through signaling pathways. Magnesium has a key role in DNA, RNA and protein synthesis, while Mg-substituted CaPs increase osteoblast cellular attachment, proliferation, and ALP production (Mammoli, 2019; Bose et al., 2013). ALPs are glycosyl-phosphatidylinositol-anchored Zn^{2+}-metallated glycoproteins that are released during the maturation process of the osteoblastic cell life cycle, which creates an alkaline environment that favors the CaP precipitation and subsequent mineralization of the ECM (Bose et al., 2013). Hwan Park et al. reported that zinc exerts osteogenic effects in hMSCs by activation of Runt-related transcription factor 2 (Runx2) *via* the cAMP-PKA-CREB signaling pathway. Both, ALP and Runx2 are highly important in hMSC differentiation to osteoblasts, which points crucial role of zinc in bone formation. (Park et al., 2018).

Recently, selenium attracted attention as a substituent in CaPs due to the selective effect on healthy and osteosarcoma cells. Selenium induces oxidative stress in cancer cells by generating reactive oxygen species and suppresses RANKL-induced osteoclastogenesis through inhibition of signaling pathways while having a positive effect on healthy osteoblast cells (Yang et al., 2011). In accordance with our previous study (Ressler et al., 2021) the composite scaffolds, with SeO_3^{2-} substituted CaP, revealed anticancer properties on U2OS cells, while at the same time enhancing the proliferation of healthy HEK 293 cells (data not shown). The obtained results are in agreement with results reported by Uskoković et al., where biomaterial substituted with selenium has selective toxicity for osteosarcoma cells,

while not affecting the viability of non-cancerous primary cells. (Uskoković, Iyer, & Wu, 2017).

In the present work hMSCs seeded on the composite scaffolds were evaluated after 14 and 21 days of cell culture. The biological evaluation was carried out at static and dynamic conditions using a perfusion bioreactor. The histological, immunohistochemical and RT-qPCR analyses were used to determine the osteogenic properties of prepared scaffolds. Detection of a higher amount of newly-formed bone tissue, ALP, BSP, COLL I, DMP1 and phosphate doposits, characteristic for differentiation process, indicate good osteogenic signal of the scaffolds substituted with trace elements, especially the scaffolds with the synergic effect of ions, SC_1MIX and SC_5MIX. The hMSCs differentiated in osteoblasts phenotype within 21 days of cell culture indicating the possible application of SC_1MIX and SC_5MIX as scaffolds for bone tissue regenerative applications.

As the single substituent systems have demonstrated good results in recent studies, using multiple substituents can be used to further increase the beneficial effects of each. A combination of different trace metal ion additions in CaPs can alter the degradation kinetics, the inhibitory effect on osteoclastogenesis, and the stimulatory effect on osteogenesis (Bose et al., 2013). This research highlight the key role of trace elements and their synergic effect on hMSC differentiation and the formation of newly-bone tissue. Trace elements have shown that they have potential to replace growth factors and pharmaceologics for enhancing the regenerative properties of synthetic materials without causing negative side effects. However, further *in vivo* studies on animal models need to be performed to examine biodegradation and osteogenesis to confirm the applicability of the SC_5MIX scaffold for bone tissue engineering.

5. Conclusion

Present research has shown that multi-substituted scaffolds based on chitosan and CaP, mainly composed of HAp, acts as three-dimensional support for hMSCs proliferation and differentiation into osteoblast cells. Expression of characteristic bone genes, ALP, BSP, COLL I, DMP1 and phosphate deposits, along with newly formed bone tissue, indicated that ECM mineralization took place during 21 days of hMSCs culture indicating the key role of Sr^{2+}, Mg^{2+}, Zn^{2+} and SeO_3^{2-} during osteogenesis. Prepared scaffolds are highly stable under physiological and enzymatic conditions even the natural polymer chitosan was used.

Acknowledgments

The financial supports of the European Regional Development Fund (grant KK.01.1.1.07.0014.), the PID2019-106000RB-C21/AEI/10.13039/501100011033 project from rhe Spanish Research Agency, and the L'Oréal-UNESCO Foundation 'For Women in Science' are gratefully acknowledged.

References

Aubin, J. E., Chapter 4 - Mesenchymal Stem Cells and Osteoblast Differentiation, Ed: John P. Bilezikian, Lawrence G. Raisz, T. John Martin, Principles of Bone Biology (Third Edition), Academic Press, 2008, Pages 85–107, doi: 10.1016/B978-0-12-373884-4.00026-4

Boanini, E., Gazzano, M., Bigi, A. (2010). Ionic substitutions in calcium phosphates synthesized at low temperature, *Acta Biomaterialia*, 6 1882–1894. doi: 10.1016/j.actbio.2009.12.041

Bonnelye, E., Chabadel, A., Salterl, F., Jurdic, P. (2008). Dual effect of strontium ranelate: stimulation of osteoblast differentiation and inhibition of osteoclast formation and resorption *in vitro, Bone*, 42, 129–138. doi: 10.1016/j.bone.2007.08.043.

Bose, S., Fielding, G., Tarafder, S., Bandyopadhyay, A. (2013). Understanding of dopant-induced osteogenesis and angiogenesis in calcium phosphate ceramics, *Trends in Biotechnology*, 1, 594–605. doi: 10.1016/j.tibtech.2013.06.005

Cardonnier, T., Sohier, J., Rosset, P., Layrolle, P. (2011). Biomimetic Materials for Bone Tissue Engineering – State of the Art and Future Trends, *Advanced Engineering Materials*, 13, 135–150. doi:10.1002/adem.201080098

Deb, P., Deoghare, A.B., Borah, A., Barua, E., Das Lala, S. (2018). Scaffold Development Using Biomaterials: A Review, *Materials Today: Proceeding*, 5, 12909–12191. doi: 10.1016/j.matpr.2018.02.276

Dorozhkin, S.V. (2014). Calcium Orthophosphates: Occurrence, Properties and Major Applications, *Bioceramics Development and Applications*, 4, 1–20. doi: 10.4172/2090-5025.1000081

Fernandez-Yague, M.A., Abbah, S.A., McNamara, L., Zeugolis, D.I., Pandit, A., Biggs, M.J. (2015). Biomimetic approaches in bone tissue engineering: Integrating biological and physicomechanical strategies, *Advanced Drug Delivery Reviews*, 84, 1–29. doi: 10.1016/j.addr.2014.09.005

Gámiz-González, M.A., Guldris, P., Antolinos Turpín, C.M., Ródenas Rochina, J., Vidaurre, A., Gómez Ribelles, J.L. (2017). Fast degrading polymer networks based on carboxymethyl chitosan, *Materials Today Communications*, 10, 54–66. doi: 10.1016/j.mtcomm.2017.01.005

Golub, E.E., Boesze-Battaglia, K., (2007). The role of alkaline phosphatase in mineralization, *Current Opinion in Orthopaedics*, 18, 444–448 doi: 10.1097/BCO.0b013e3282630851

Gordon, J.A.R., Tye, C.E., Sampaio, A.V., Underhill, T.M., Hunter, G.K., Goldberg, H.A. (2007). Bone sialoprotein expression enhances osteoblast differentiation and matrix mineralization *in vitro*, *Bone*, 41, 462–473. doi: 10.1016/j.bone.2007.04.191.

Hou, Y.P., Hu, J.L., Park, H., & Lee, M. (2012). Chitosan-based nanoparticles as a sustained protein release carrier for tissue engineering applications, *Journal of Biomedical Materials Research A*, 100, 939–944. doi: 10.1002/jbm.a.34031.

Kalajzic, I., Braut, A., Gui, D., Jiang, X., Kronenberg, M.S., Mina, M., Harris, M.A., Rowe, D.W. (2004). Dentin matrix protein 1 expression during osteoblastic differentiation, generation of an osteocyte GFP-transgene, *Bone*, 35, 74–82. doi: 10.1016/j.bone.2004.03.006.

Kalantari, K., Afifi, A.M., Jahangirian, H., Webster, T.J. (2019). Biomedical applications of chitosan electrospun nanofibers as a green polymer – Review, *Carbohydrate polymers*, 207, 588–600. doi: 10.1016/j.carbpol.2018.12.011

Karageorgiou, V., Kaplan, D. (2005). Porosity of 3D biomaterial scaffolds and osteogenesis, *Biomaterials*, 26, 5474–5491. doi: 10.1016/j.biomaterials.2005.02.002

Kirkham, G.R., Cartmell, S.H., (2007) Genes and Proteins Involved in the regulation of osteogenesis, *Topics in Tissue Engineering*, 3, 20.

Kulterer, B., Friedl, G., Jandrositz, A., Sanchez-Cabo, F., Prokesch, A., Paar, C., Scheideler, M., Windhager, R., Preisegger, K.H., Trajanoski, Z. (2007). Gene expression profiling of human mesenchymal stem cells derived from bone marrow during expansion and osteoblast differentiation, *BMC Genomics*, 8, 70. doi: 10.1186/1471-2164-8-70.

Matić, I., Antunović, M., Brkić, S., Josipović, P., Čaput Mihalić, K., Karlak, I., Ivković, A., Marijanović, I., (2016). Expression of OCT-4 and SOX-2 in bone marrow- derived human

mesenchymal stem cells during osteogenic differentiation, *Open access Macedonian journal of medical sciences*, 4, 9–16. doi: 10.3889/oamjms.2016.008

Mavrogenis, A.F., Dimitriou, R., Parvizi, J., Babis, G.C. (2009). Biology of implant osseointegration, *Journal of Musculoskeletal and Neuronal Interactions*, 9, 61–71.

Mammoli, F., Castiglioni, S., Parenti, S., Cappadone, C., Farruggia, G., Iotti, S., Davalli, P., Maier, J.A.M., Grande, A., Frassineti, C. (2019). Magnesium Is a Key Regulator of the Balance between Osteoclast and Osteoblast Differentiation in the Presence of Vitamin D3, *International Journal of Molecular Sciences*, 20, 385. doi: 10.3390/ijms20020385

Minardi, S., Corradetti B., Taraballi F., Sandri M., Van Eps J,. Cabrera F.J., Weiner B.K., Tampieri A., Tasciotti E. (2015). Evaluation of the osteoinductive potential of a bio-inspired scaffold mimicking the osteogenic niche for bone augmentation, *Biomaterials*, 62, 128–137. doi: 10.1016/j.biomaterials.2015.05.011.

Morales-Román, R.M., Guillot-Ferriols, M., Roig-Pérez, L., Lanceros-Mendez, S., Gallego-Ferrer, G., Gómez Ribelles, J.L. (2019). Freeze-extraction microporous electroactive supports for cell culture, *European Polymer Journal*, 119, 531–540. doi: 10.1016/j.eurpolymj.2019.07.011

Muzzarelli, R.A.A. (2011). Chitosan composites with inorganics, morphogenetic proteins and stem cells, for bone regeneration, *Carbohydrate polymers*, 83, 1433–1445. doi: 10.1016/j.carbpol.2010.10.044

Park, K.H., Choi, Y., Yoon, D.S., Lee, K.M., Kim, D., Lee, J.W. (2018). Zinc Promotes Osteoblast Differentiation in Human Mesenchymal Stem Cells Via Activation of the cAMP-PKA-CREB Signaling Pathway, *Stem Cells and Development*, 27, 1125–1135. doi: 10.1089/scd.2018.0023.

Postmann, B., Jung, K., Schmechta, H., Evers, U., Pergande, M., Porstmann, T., Kramm, H.J., Krause, H. (1989). Measurement of lysozyme in human body fluids: Comparison of various enzyme immunoassay techniques and their diagnostic application, *Clinical Biochemistry*, 22, 349–355. doi: 10.1016/S0009-9120(89)80031-1

Ren, D., Yi, H., Wang, W., Ma, X. (2005). The enzymatic degradation and swelling properties of chitosan matrices with different degrees of N-acetylation, *Carbohydrate Research*, 340, 2403–2410. doi:10.1016/j.carres.2005.07.022

Ressler, A. (2020). Biomaterials based on chitosan and metal-ion-substituted hydroxyapatite for tissue engineering applications (Doctoral thesis). Faculty of Chemical Engineering and Technology, University of Zagreb.

Ressler, A., Antunović, M., Cvetnić, M., Ivanković, M., Ivanković, H. (2021). Selenite Substituted Calcium Phosphates: Preparation, Characterization, and Cytotoxic Activity, *Materials*, 14(12), 3436. doi: 10.3390/ma14123436

Ressler, A., Cvetnić, M., Antunović, M., Marijanović, I., Ivanković, M., Ivanković, H. (2020a). Strontium substituted biomimetic calcium phosphate system derived from cuttlefish bone, *Journal of Biomedical Materials Research: Part B Applied Biomaterials*, 108, 1697–1709. doi: 10.1002/jbm.b.34515

Ressler, A., Gudelj, A., Zadro, K., Antunović, M., Cvetnić, M., Ivanković, M., Ivanković, H. (2020b). From Bio-waste to Bone Substitute: Synthesis of Biomimetic Hydroxyapatite and Its Use in Chitosan-based Composite Scaffold Preparation, *Chemical and Biochemical Engineering Quarterly*, 34, 59-71. doi: 10.15255/CABEQ.2020.1783

Ressler, A., Ródenas-Rochina, J., Ivanković, M., Ivanković, H., Rogina, A., Gallego Ferrer, G. (2018). Injectable chitosan-hydroxyapatite hydrogels promote the osteogenic

differentiation of mesenchymal stem cells, *Carbohydrate Polymers*, 197, 469–477. doi: 10.1016/j.carbpol.2018.06.029

Roseti, L., Parisi, V., Petretta, M., Cavallo, C., Desando, G., Bartolotti, I., Grigolo, B. (2017). Scaffolds for Bone Tissue Engineering: State of the art and new perspectives, *Materials Science and Engineering: C*, 78, 1246–1262. doi: 10.1016/j.msec.2017.05.017

Rogina, A., Antunović, M., Pribolšan, L., Caput Mihalić, K., Vukasović, A., Ivković, A., Marijanović, I., Gallego Ferrer, G., Ivanković, M., Ivanković, H., (2017). Human Mesenchymal Stem Cells Differentiation Regulated by Hydroxyapatite Content within Chitosan-Based Scaffolds under Perfusion Conditions, *Polymers*, 9, 387–404. doi: 10.3390/polym9090387

Rogina, A., Rico, P., Gallego Ferrer, G., Ivanković, M., Ivanković, H. (2015). In Situ hydroxyapatite content affects the cell differentiation on porous chitosan/ hydroxyapatite scaffolds, *Annals of Biomedical Engineering*, 44, 1107. doi: 10.1007/s10439-015-1418-0

Sanmartín-Masiá, E., Poveda-Reyes, S., Gallego Ferrer, G. (2017). Extracellular matrix–inspired gelatin/hyaluronic acid injectable hydrogels, *International Journal of Polymeric Materials and Polymeric Biomaterials*, 66, 280–288. doi: 10.1080/00914037.2016.1201828

Seibel, M.J., (2005). Biochemical Markers of Bone Turnover Part I: Biochemistry and Variability, *Clinical Biochemist Reviews*, 26, 97–122.

Suzuki, O., Kamakura, S., Katagiri, T., Nakamura, M., Zhao, B., Honda, Y., Kamijo, R. (2006). Bone formation enhanced by implanted octacalcium phosphate involving conversion into Ca-deficient hydroxyapatite, *Biomaterilas*, 27, 2671–2681. doi: 10.1016/j.biomaterials.2005.12.004

Yang, F., Yang, D., Tu, J., Zheng, Q., Cai, L., Wang, L. (2011). Strontium enhances osteogenic differentiation of mesenchymal stem cells and in vivo bone formation by activating Wnt/catenin signaling, *Stem Cells*, 29, 981–991. doi: 10.1002/stem.646.

Uskoković, V., Iyer, M.A., Wu, V.M., (2017). One ion to rule them all: the combined antibacterial, osteoinductive and anticancer properties of selenite-incorporated hydroxyapatite, *Journal of Materials Chemistry B*, 5, 1430–1445. doi: 10.1039/C6TB03387C

Venkatesan, J., Kim, S.K. (2010). Chitosan Composites for Bone Tissue Engineering—An Overview, *Marine Drugs*, 8, 2252–2266. doi: 10.3390/md8082252

Graphical abstract